REPORT DOCUMENTATION PAGE

AFRL-SR-AR-TR-05-

0524

1. AGENCY USE ONLY *(Leave blank)*	2. REPORT DATE	3. REPORT TYPE AND DATES COVERED
	16 DEC 05	FINAL

4. TITLE AND SUBTITLE
Bio-Inspired Batteries: Using Dispersion Forces to Self-Assemble Electrochemical Devices

5. FUNDING NUMBERS
F49620-02-1-0406

6. AUTHOR(S)
Chiang, Yet-Ming

7. PERFORMING ORGANIZATION NAME(S) AND ADDRESS(ES)
Room 13-4086
Massachusetts Institute of Technology
Cambridge, MA 02139

8. PERFORMING ORGANIZATION REPORT NUMBER

9. SPONSORING/MONITORING AGENCY NAME(S) AND ADDRESS(ES)
Jennifer Gresham
AFOSR/NL
875 North Randolph Street
Suite 325, RM 3112
Arlington, VA 22203

10. SPONSORING/MONITORING AGENCY REPORT NUMBER

11. SUPPLEMENTARY NOTES

12a. DISTRIBUTION AVAILABILITY STATEMENT
Approve for Public Release: Distribution Unlimited

12b. DISTRIBUTION CODE

13. ABSTRACT *(Maximum 200 words)*

14. SUBJECT TERMS

15. NUMBER OF PAGES

16. PRICE CODE

17. SECURITY CLASSIFICATION OF REPORT	18. SECURITY CLASSIFICATION OF THIS PAGE	19. SECURITY CLASSIFICATION OF ABSTRACT	20. LIMITATION OF ABSTRACT

Final Report for
AFOSR Grant No. F49620-02-1-0406:

Self-Organizing Batteries

December 16, 2005

Principal Investigator:

Yet-Ming Chiang
Room 13-4086
Massachusetts Institute of Technology
Cambridge, MA 02139
Tel: 617-253-6471
Email: ychiang@mit.edu

Program Manager:

Maj. Jennifer Gresham, Ph. D.
AFOSR Program Manager
Surface and Interfacial Science
875 North Randolph St.
Suite 325, Room 3112
Arlington, VA 22203

Objectives:

This research aimed to use colloidal self-organization to create complete bipolar electrochemical devices. In this approach, repulsive and attractive surface forces are introduced within device structures to form: 1) nanoscale electrochemical junctions between electronically conductive anodes and cathodes; 2) electronically conductive networks of storage materials particles; and 3) electrical connections to the external circuit via selective attachment of particles to current collectors. Rechargeable lithium batteries were used as a testbed device for this approach. In particular, efforts were aimed at enabling a self-organized architecture (Figure 1) in which a continuously percolating cathode network is "wired" to one current collector and an anode network to the other, while the two networks are isolated everywhere from one another by repulsive surface forces. Repulsive dispersion forces (negative Hamaker constant) and other surface forces were used to create permanent electrochemical junctions that upon drying or solidification of the liquid medium are filled by solid polymer electrolyte, resulting in solid-state devices. Such batteries could be economically fabricated at sizes and shapes ranging from printed microbatteries to large-scale continuous coatings, and would have increased energy and power densities due to improved packing and reduced transport distances. This work represents a fundamentally new approach to electrochemical device fabrication, ultimately applicable to a broad range of DoD technologies.

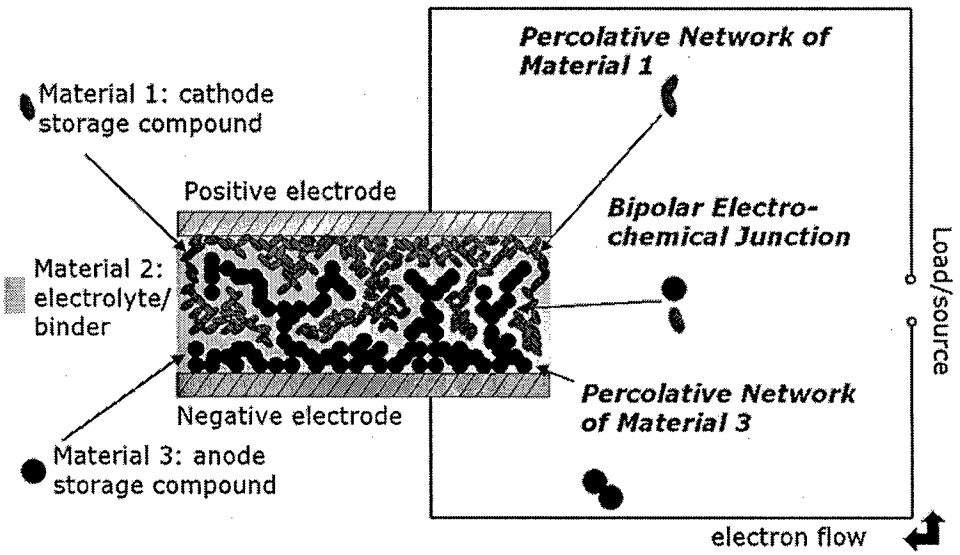

Figure 1. Colloidal self-assembly aims to replace the conventional laminated battery design with an interpenetrating electrode design.

Accomplishments:

There were two main areas of accomplishment under this program. The first was the development of new understanding, and identification of key materials and selection criteria, for electronically conductive device materials having repulsive van der Waals

forces enabling junction formation. The second was the application of these principles to a lithium ion battery, resulting in the demonstration of the first self-organized rechargeable battery. These accomplishments are described separately below.

1. Short-Range Repulsive Forces between Conductive Device Materials

In this part of the project, our goals were the following:

- Identification of negative Hamaker constant materials systems for self-organization. From theory and experiment, indium tin oxide (ITO) has been identified as one of a group of "low-index," *electronically conductive* endmembers that exhibit repulsive van der Waals force against high-index conductive materials such as graphite or metals. This is a new accomplishment in the field of surface forces, where all previous negative Hamaker systems have been insulators that are not useful as active device materials. This discovery solves the hardest materials selection problem for self-organization. The widespread applicability of ITO as a conductive electrode material suggests that it can be used in variety of self-organized electrochemical devise (e.g., electrochromics as well as batteries). ITO has also been found to be electrochemically stable in lithium battery electrolytes and to conduct/store lithium.
- Demonstration of junction formation in solid-polymer electrolyte containing systems. Between particle suspensions of dissimilar electronically conductive materials (ITO and graphite), each of which forms a continuous (percolating) particle network and are lithium storage compounds, the resistive junction formed via repulsive surface forces between the mobile suspensions was preserved after complex processing/drying phenomena, resulting in solid-polymer electrolyte separated junctions.
- The stability of junctions formed by the current approach at working voltages typical of lithium ion batteries (4V) was demonstrated (i.e., absence of shorting).

Materials Selection and Design. The most challenging materials selection/design task has been to find suitable "low-index" endmembers of the dispersion-force couple. This material must provide a repulsive dispersion force when used against the "high-index" endmember, of which there are many candidates, and must also be electronically and ionically conductive. This material could be used as an active material or as a coating for an active material (e.g., as a coating for an otherwise desirable storage material that has high-index). We subsequently carried out a re-examination of the dielectric and optical properties for a broad range of electronically conductive oxides, including lithium intercalation oxides, and calculated dispersion forces using the full spectral range of dielectric response wherever available. Figure 2 illustrates the approach for one combination of materials with negative Hamaker constant. This study revealed that several highly conductive systems that might have been considered suitable only as the high-index endmember, instead had spectral properties in the UV (which dominates the dispersion interaction) that cause them to act as the low-index endmember. Of these, indium tin oxide (ITO) emerged as a leading candidate due to its exceptionally high electronic conductivity, ~500 S/cm at room temperature, its good lithium conductivity,

and its ability to intercalate lithium at a potential (with respect to lithium metal) of ~0.5V. The latter properties were directly verified using standard electrochemical tests. Thus ITO is highly suitable for use as an anode or as a coating for other anodes or cathodes to provide the desired repulsive dispersion force.

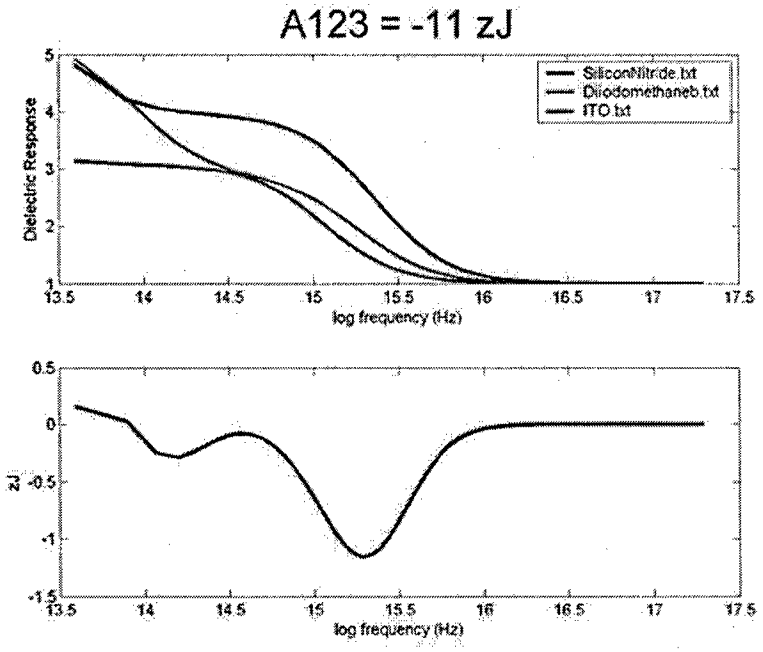

Figure 2. Dielectric response vs. frequency for three materials, and the spectrally-resolved Hamaker constant. Silicon nitride is here the high-index endmember, while ITO is the low-index endmember. Note that the solvent has a dielectric response in between that of the two solids over a wide range of frequencies, giving a negative Hamaker constant. (The UV range 10^{15}-10^{16} Hz plays the most important role however).

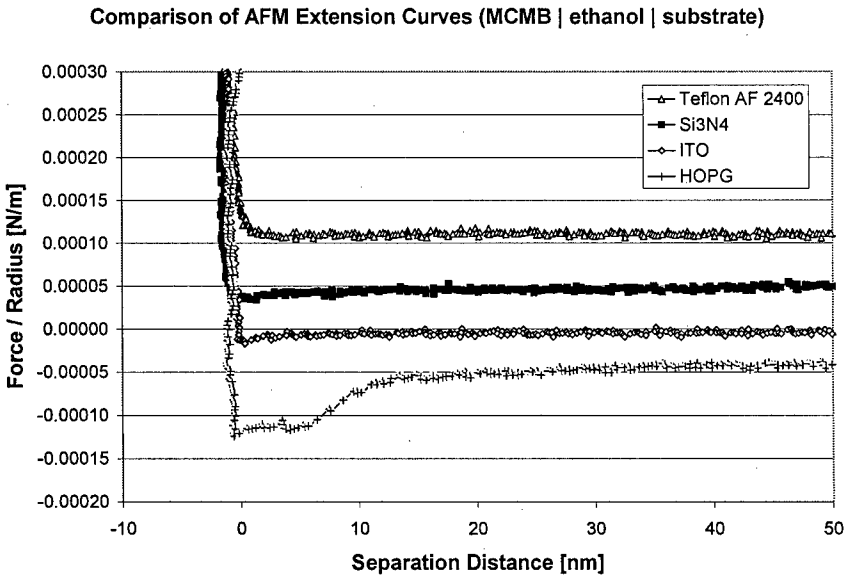

Figure 3. AFM extension curves for an MCMB tip against four substrate materials in ethanol solvent. The spectra are slightly offset on the displacement axis for readability. Only in the case of HOPG is there significant attraction.

To directly observe the force between dissimilar solids in a liquid medium, we used wet-cell atomic force microscopy (AFM). MCMB (mesocarbon microbeads), a spherical graphite widely used as a lithium ion battery anode, was used as the high-index endmember and was attached to an AFM cantilever. Its interaction with a film of an opposing material was measured while both were immersed in solvents that varied in dielectric response as well as polar/nonpolar character. Figure 3 shows the AFM extension curves for MCMB vs. four solids in ethanol solvent. Here an attraction is seen between the MCMB and highly-oriented pyrolytic graphite (HOPG), while the interaction is repulsive or near-zero between MCMB and the other three materials, including ITO. From numerous such experiments we then focused on MCMB vs. ITO as a model system which exhibits repulsive surface forces in several solvents, of which acetonitrile, m-xylene, and ethanol received the most attention.

Surface Force Induced Electrical Isolation Between Dissimilar Materials. Subsequent experiments explored whether the observed repulsive surface forces measured by AFM resulted in electronic separation between the two conductive solids. In order to transition between single-particle measurements and multiparticle devices, we performed measurements on "instrumented" suspensions of particles. Figure 4 illustrates one successful experimental configuration. Electrodes of platinum and ITO, representing high-index and low-index endmembers (or current collectors) respectively, were used to measure the conductivity of particle suspensions. Impedance spectroscopy was used to measure the response of the system. Figure 4 shows results for a suspension of MCMB particles in m-xylene. When both electrodes are Pt, a resistance of $\sim 5 \times 10^2\ \Omega$ is observed. (The relatively high resistance is due to the fact that the MCMB particles, are undergoing Brownian motion.) Upon substituting an ITO electrode for one Pt electrode, however, the resistance immediately increases to $\sim 5 \times 10^4\ \Omega$. Introducing a second ITO electrode further increases the resistance, by about a factor of 2. Thus the interface between ITO and the MCMB suspension is shown to have $\sim 5 \times 10^4\ \Omega$ greater resistance than that between the Pt and MCMB suspension. We attribute this increase in resistance to the repulsive surface force between ITO and MCMB.

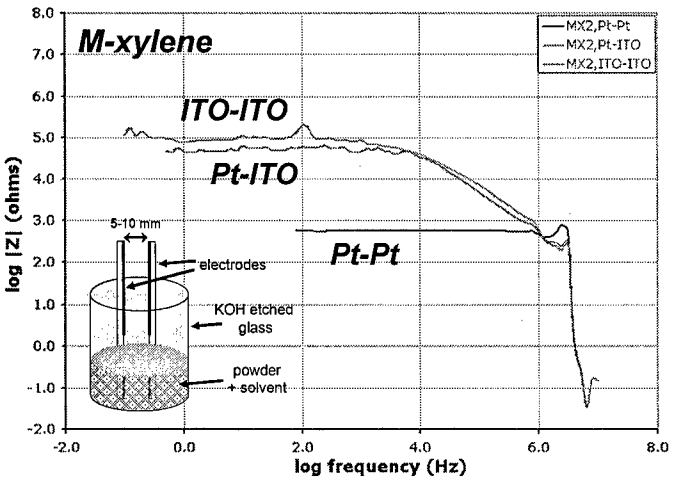

Figure 4. Impedance spectroscopy measurements of the resistance of an MCMB suspension in m-xylene, between Pt or ITO electrodes.

Introducing Solid-Polymer Electrolytes into Surface-Force Separated Systems. Having shown that repulsive surface forces measured by AFM do result in a marked increase in electronic conductivity between ITO and MCMB, we next faced the challenge of preserving the electronically isolated materials in an all solid-state system, and demonstrating that the resulting junctions could be stable under electrochemical conditions typical of lithium ion battery systems. We used PEO + $LiClO_4$ as our model solid polymer electrolyte system, and acetonitrile as a model solvent due to its ability to dissolve both. Indeeed, acetonitrile is a preferred solvent for processing the PEO family of solid electrolytes. Several hundred suspensions of ITO and MCMB were prepared, exploring the parameter space of solid/solvent ratio and polymer/salt concentration, in order to determine the conditions under which the following could be achieved:

- A coagulating or nearly-coagulating suspension; i.e., one in which the like particles of MCMB or ITO are not stabilized by strong repulsive forces due to electrostatic or steric stabilization.
- Drying of the individual MCMB or ITO suspensions to form an electronically percolating suspension with all pore space filled by PEO electrolyte.
- A ratio of PEO to $LiClO_4$ that results in good lithium conductivity

Once these suspension formulations were developed, we conducted experiments in which MCMB and ITO suspensions were placed into direct contact while wet, and allowed to dry to form particle networks embedded within solid PEO electrolyte. The configuration is illustrated in Figure 5. Upon drying, the resistance of each dried suspension was measured with a 2-point measurement, as well as the resistance between the two conductive suspensions. Numerous drying conditions were explored. As shown in Figure 5, for certain combinations of suspension formulation and drying conditions we obtained large electrical resistances (4 MΩ) between conductive suspensions.

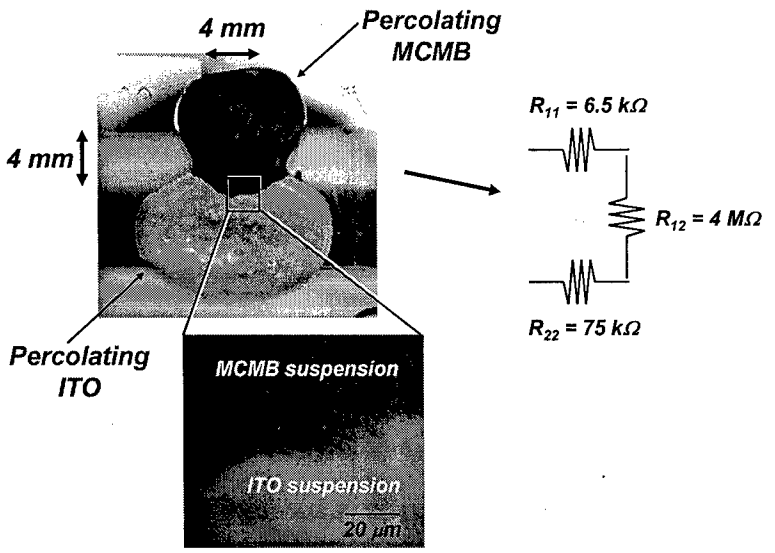

Figure 5. Suspensions of MCMB and ITO respectively, in acetonitrile + PEO + $LiClO_4$ solution, were placed in contact while wet and allowed to dry. Highly insulating interfaces formed between the conductive suspensions.

Finally, we tested the stability of the insulating interface between the ITO and MCMB at potentials up to 4V, the working voltage of typical lithium ion batteries. Figure 6 shows cyclic voltammetry results at a variety of temperature, for sample of the configuration in Figure 5. It was seen that up to 4V, no electrical breakdown is observed, the resistance remaining ~2 MΩ even at the highest voltage of 4V.

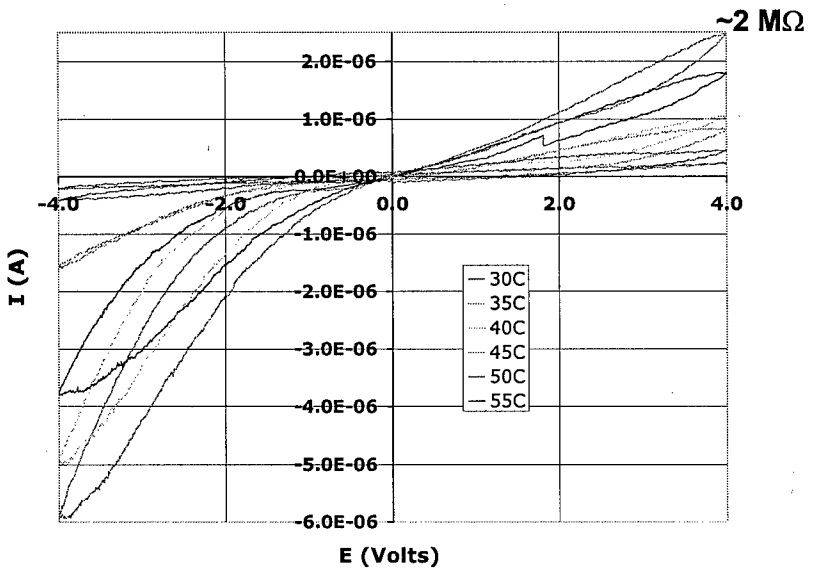

Figure 6. Cyclic voltammetry of a sample as in Figure 5, measured between the two suspensions so as to determine the stability of the highly resistive interface between the suspensions. No breakdown is observed up to 4V.

The above-described work has now been completed, and is being prepared for publication.

2. *Development of a Colloidal-Scale Self-Organizing Lithium Rechargeable Battery*

In this part of the project, $LiCoO_2$ and graphite were used as the active materials for a lithium rechargeable battery, and solvent systems were identified in which the desired short-range repulsive forces exist. This work followed the methodology described above, and culminated in the demonstration of the first self-organized lithium rechargeable battery. This work has now been submitted for publication, and is attached as Appendix 1.

Personnel Supported:

Yet-Ming Chiang, Professor, Department of Materials Science and Engineering
Steven M. Tobias, Research Assistant, Dept of Materials Science and Engineering
Dr. Young Kyu Cho, Postdoctoral Associate, Dept. of Materials Science and Engineering

Publications:

"Colloidal-Scale Self-Organizing Lithium Batteries,"Young Kyu Cho, Ryan Wartena, Yet-Ming Chiang, submitted.

"Investigation of Short-Range Surface Forces to Develop Self-Organizing Devices," Steven M. Tobias, S.M. Thesis, MIT, 2004.

Interactions/Transitions:

Invited Presentations:

"Towards 3D Nanobatteries: Self-Organization of Electrochemical Devices from Heterogeneous Colloids," Nano Materials for Defense Applications Symposium, Maui, HI, February 23-26, 2004.

"Self-Assembling Batteries," TTI/Vanguard Conference: Powering the Future, Montreal, Canada, April 19-20, 2004.

"Ceramics in Advanced Battery Technology," Technology Roadmapping Symposium, The American Ceramic Society, Indianapolis, IN, April 21, 2004.

"Self-Organization of Micro- and Nanoscale Electrochemical Devices from Heterogeneous Suspensions," Asian Solid State Ionics Meeting, Jeju, Korea, June 6-11, 2004.

"New Directions in Device Design for Lithium Batteries," International Meeting on Lithium Batteries 12, Nara, Japan, July 1, 2004.

"Using Surface Forces to Self-Organize Electrochemical Devices from Heterogenous Colloids, International Workshop on Interfaces," Santiago de Compostela, Spain, June 2005

"Self-Organized Batteries," The Electrochemical Society Fall Meeting, 2005.

Transitions: Patent applications held by MIT on this approach have been licensed by A123Systems of Boston, MA. Contact individual: Dr. Bart Riley, VP of R&D, 8 Saint Mary's St, Boston, MA 02215, 617-778-5700.

New Discoveries, Inventions, or Patent Disclosures:

Patent applications submitted during contract:

"Electrophoretic Assembly of Electrochemical Devices," Yet-Ming Chiang, Dong-Wan Kim, Steven M. Tobias, Benjamin Hellweg, and Richard K. Holman, U.S. Patent Applications, June 2004.

Appendix 1: Submitted Paper

Colloidal-Scale Self-Organizing Lithium Batteries

Young Kyu Cho,[1] Ryan Wartena,[1] Yet-Ming Chiang[2]
Massachusetts Institute of Technology
Cambridge, MA 02139

[1]These authors contributed equally to this work. [2]Corresponding author,
ychiang@mit.edu

Abstract

Since Volta (*1*), batteries and other electrochemical devices have been fabricated by the manual assembly of critical components. The advent of distributed and autonomous electronics requiring very small and high energy density power sources, as well as continuing demand in larger batteries for low cost energy and power, has created a need for entirely new fabrication approaches. We show that nanoscale electrochemical junctions can be formed between dissimilar electrodes using short-range repulsive interactions alone, and when combined with formation of percolating particle networks using attractive interactions, results in self-organizing and self-wiring devices. Lithium rechargeable batteries using $LiCoO_2$ and graphite as active materials are demonstrated. Force microscopy is used to measure interactions between electrode materials. Electrochemical functionality of junctions formed by surface forces alone, and repeated cycling of a self-organized wet-cell rechargeable battery, are presented. A new general approach to direct formation of bipolar devices from heterogeneous colloids is suggested.

Advances in nanotechnology have resulted in numerous devices that utilize contact-junctions between nanoscale materials, including bi-stable carbon nanotube memory, diodes, light-emitting diodes (LEDs), logic gates, and solar cells (*2-5*). Attractive van der Waals forces provide the intimate contact allowing electron transport across these nanoscale ohmic and *pn* junctions. In contrast, bipolar electrochemical devices such as batteries, fuel cells, electrochromic displays, and certain types of sensors are fundamentally based on the separation of electronically conducting electrodes by ionically conducting but electronically insulating electrolytes. Beginning with the original work by Volta (*1*), these devices have and continue to be fabricated from separate cathode and anode materials along with their current collectors, separator films, and electrolytic layers through multiple steps. Current devices ranging in length scale from microns-thick thin film microbatteries (*6,7*), to lithium rechargeable batteries based on wound microlaminates of 50-100 μm thickness (*8*), to the macroassemblies used in common alkaline and lead-acid batteries. Two converging needs drive the work presented here. First, as the size scale of powered devices continues to shrink, there is a clear and growing need for distributed high energy density power sources of comparable size scale. Currently recognized applications include autonomous microelectromechanical systems (MEMS), implantable medical devices, remote sensing and communications, and nano/molecular electronics (*9,10*). Second, the laminated construction of current high energy density batteries (e.g., lithium-ion), now approaching its engineering limits, has inefficient mass and volume utilization, with only 30-40% of the available device volume being used for ion storage (*11*). Attempts to increase power density, for instance by using thinner electrodes, invariably come at the expense of

energy density. New, more efficient device designs and fabrication approaches (*12*) are needed in order to break free of these constraints.

One recent path to microbatteries has followed the "top-down" approach using various forms of microfabrication (*6,7,10,13,14*). Here we demonstrate for the first time a "bottom-up" approach to battery fabrication that simultaneously uses repulsive and attractive forces between colloidal-scale ion storage materials to self-organize complete bipolar devices. This self-organization scheme is illustrated in Fig. 1 for several device constructions. In each instance, repulsion between cathode and anode is used to form the critical electrochemical junction, the nanoscale gap being filled by an ionic conductor that negates the need for a separately inserted electrolyte. Concurrently, attraction (adhesion) between particles of a single type, and between an electrode material and its current collector, can be used to accomplish several functions. At the smallest size scale, selective adhesion of the materials to their respective current collectors would allow the self-organization of a battery having a single pair of particles or nanorods (Fig. 1A, 1B) (*15*). For multiparticle devices of various size scales, it is necessary to join active materials of a single type into electronically-percolating networks that are everywhere insulated from the opposing electrode (Fig. 1C). A natural extension is the self-organizing device shown in Fig. 1D, where co-continuous interpenetrating networks of cathode and anode form from a single heterogenous colloid, creating a two-dimensional or three-dimensional interpenetrating electrode battery (*12*). With properly tuned intereactions, a single heterogeneous suspension could be used to produce printable, self-organizing batteries at various size scales. The interpenetrating electrode design also has

fundamental performance advantages compared to conventional laminated batteries, including higher rate capability or the ability to use active materials of lower intrinsic conductivity, due to reduction of the ion transport length to the single particle scale (<1 μm, similar to thin film batteries). Higher energy density due to better volumetric utilization of the available space by densely-packed particles may be possible, since packing densities in excess of 60 vol% are achievable in many particle suspensions. Heterogeneous colloids having the prescribed interparticle potentials (repulsion between dissimilar particles, attractive between like) are inherently phase-separating systems whose ground state is two bulk phases. Thus the scheme in Fig. 1D is a partially phase-separated colloid trapped in a metastable state, and should form structures analogous to phase-separated materials (*16*). This form of colloidal ordering may be viewed as the inverse of "ionic colloidal crystals" in which electrostatic attraction between oppositely-charged particles results in ordered structures analogous to ionic crystals (*17*). We note also an earlier example of mesoscale self-assembly using simultaneous attractive and repulsive (hydrophobic and hydrophilic) surfaces (*18*), there applied to anisometric "tiles" of a single material to create a range of self-assembled structures.

Derjaguin-Landau-Verwey-Overbeek (DLVO) theory (*19*) and its many refinements inform that interparticle forces of various origins and length scales have combined effects that together determine adhesive or repulsive interactions between condensed phases. We first searched for cathode-solvent-anode combinations for which there exists a short-range repulsion, and tested the ability of the junctions to withstand typical 3-4V operating voltages. Repulsive London dispersion (LD) forces (*20-27*) are one such short-range

interaction, known to influence phenomena such as polymer phase separation (*21*), particle rejection from crystallization fronts (*22*), and cell adhesion (*23*). Repulsion occurs for materials combinations where the Hamaker constant between any two phases 1 and 3 separated by a medium 2, here denoted A_{123}, has a negative value. This requires that the dielectric response of material 2 lies between that of materials 1 and 3 over a sufficiently wide frequency range (generally emphasizing the ultraviolet); A_{123} can be determined from optical and dielectric properties (*28*) or rigorously calculated from Lifshitz theory (*29*) given sufficient frequency-dependent dielectric data for all the materials. Prior experimental work (*26,27*) has typically used Teflon™ as the "low index" endmember. To our knowledge repulsive LD forces between highly electronically conductive device materials have not previously been characterized; indeed selection of the low-index endmember is expected to be difficult given that most good conductors are high-index materials. We are not aware of any previous work in which the repulsive LD force has been used in a device application.

One useful low-index endmember was recently identified to be indium tin oxide (ITO), as it has a dielectric response providing negative A_{123} when used against high-index conductors with organic solvents of intermediate dielectric response (*30*). Repulsive interactions were experimentally confirmed. ITO is a possible current collector material for the devices of Fig. 1. (*31*) However, for common lithium storage cathodes such as $LiCoO_2$, insufficient optical data exists for the quantitative evaluation of Hamaker constants. Thus we experimentally tested, using wet-cell atomic force microscopy (AFM), the short-range interactions between $LiCoO_2$ and graphite in a range of solvents.

Particles of $LiCoO_2$ and MCMB graphite were mounted on silicon nitride cantilevers as tips (Fig. 2F), and particulate or sintered $LiCoO_2$ and highly-oriented pyrolytic graphite (HOPG) as used as substrates. The solvents were limited to those in which common lithium conducting salts such as lithium perchlorate and lithium triflate and polyethylene glycol (PEG) and polyethylene oxide (PEO) are soluble, to facilitate later incorporation of solid polymer electrolytes.

Figures 2A and 2B compare force-separation curves between MCMB tips and $LiCoO_2$ substrates measured in pure methyl ethyl ketone (MEK) and acetonitrile (AN). It is seen that MEK provides a short-range repulsion between the two active materials, while acetonitrile results in the hysteresis characteristic of adhesion. The interactions between the like materials, an MCMB tip and HOPG substrate and a $LiCoO_2$ tip and substrate, were found to be adhesive as seen in Fig. 2C and 2D, respectively. These results are consistent with the LD interaction being dominant; the dispersion force is attractive for any symmetric materials combination (positive A_{121} and A_{323}). The MCMB and $LiCoO_2$ particles are not smoothly spherical but have protrusions resulting in a sharper contact radius (Fig. 2F) than the apparent particle radius, thus some variability in the force spectra were seen with different tips. Upon fitting the curve in Fig. 2A to the force law for a contacting sphere of 0.5 μm radius against a flat plate (*20*), a reasonable value of $A_{123} = -10$ zJ is obtained. It is also known that the relative Lewis acid –Lewis base nature of contacting materials provides additional short-range interactions that can be attractive or repulsive (*32*), hence a more detailed interpretation requires evaluation of these effects in addition to the LD interaction.

Integration of the force-separation curve in Fig. 2A yields an energy barrier of ~10^{-18}J, more than 100 times the kinetic energy of ~5 μm sized graphite or $LiCoO_2$ particles at room temperature. For nanoscale particles, the surface forces would be even more dominant. Forces of this magnitude can plausibly stand off the MCMB graphite particles from the $LiCoO_2$ surface to a separation of several nanometers. The addition of $LiClO_4$ at 0.1M concentration (producing lithium ion conductivity) extended very slightly the force-separation curve, Fig. 2A. Since the ionic strength of the medium at this salt concentration should be more than sufficient to collapse any electrostatic double layer present (i.e., the Debye length κ^{-1} is less than 0.5 nm), the largely unchanged repulsion curve suggests that electrostatic effects are not significant, further supporting a dominant role of short-range interactions. We then investigated the effects of adding polyethylene glycol (PEG 1500) at 10 wt ppm and 1 wt % concentrations to MEK (Fig. 2E). At 10 ppm PEG, the range of the repulsive interaction was extended slightly to about 10nm. At 1 wt% PEG, oscillatory interactions were observed suggesting adsorption of the PEG on one or both surfaces, but the range of the interaction did not change appreciably. Both salt and polymer additions may be beneficially increase the repulsive force between $LiCoO_2$ and graphite. For the self-organization schemes of Fig. 1, it is also important that aggregation under the attractive interactions of Fig. 2B and 2C not be impaired by the addition of salt and polymer. This was confirmed by AFM measurements (not shown), and direct electrical measurements of the particle suspensions as discussed later.

A first test of junction formation measured the appearance of a finite OCV as the $LiCoO_2$ and MCMB were brought into physical contact in the presence of the solvent mixtures. Figure 3B shows results in which a sintered $LiCoO_2$ electrode was pushed into beds of MCMB particles, settled from acetonitrile and MEK suspensions respectively. In acetonitrile, when the two solids are brought into contact the OCV drops within a few seconds to zero and remains short-circuited. By contrast, in MEK there is an initial voltage drop followed by an increase in OCV towards the initial value (Fig. 3B). This behavior suggests a re-arrangement of the graphite particles at the interface with $LiCoO_2$ under the influence of short-range forces, and provided direct evidence of electrochemical junction formation between cathode and anode. (*33*)

A three-electrode wet-cell design was then used to perform detailed electrochemical tests, using $LiClO_4$ and PEG doped solutions of MEK as the liquid. A sintered bar of $LiCoO_2$ (0.55 g) was used as the positive electrode and inserted into a settled suspension of MCMB (0.28 g), Fig. 3A (short range forces between cathode and anode as shown in Fig. 2A). This cell approximates the design of the battery in Fig. 1B, with MCMB forming a percolating particle network while being everywhere repelled from the $LiCoO_2$. The third, reference electrode was made of either lithium metal or sintered $Li_4Ti_5O_{12}$, the latter being used after electrochemical lithiation to compositions providing a flat 1.55V potential (two-phase coexistence) with respect to Li metal. After the $LiCoO_2$ and MCMB suspension came to equilibrium and an OCV developed (*34*), galvanostatic charge/discharge measurements were conducted (Fig. 3C and 3D). Charging was conducted to an upper voltage limit of 4.0V, below the value (~4.3V) at which MEK

undergoes oxidative decomposion at the positive electrode. Figure 3C shows several charge/discharge cycles conducted at a current of 50 μA. After a first charge cycle to 3.0V followed by a brief hold, charging to a voltage plateau at 3.8-3.9V is seen, with ~32% of the charge capacity being recovered upon discharge between 3.5-2.7 V. An additional smaller discharge capacity seen at 2.2-2.0V is attributed to an unidentified side reaction.

The absolute potential measured at the $LiCoO_2$ and MCMB electrodes verified their Faradaic activity. Figure 3D shows reference electrode measurements conducted in the solvent mixture MEK + 0.1M $LiClO_4$ + 1 wt% PEG 1500. The reference electrode is lithium titanate, and the cell is in its 14th cycle; all data are corrected to show potentials referenced to Li/Li^+. The top curve, showing the $LiCoO_2$ potential, charges at ~4.4V and reaches 3.9V at rest, showing that the $LiCoO_2$ is indeed charged (delithiated). The MCMB potential (bottom curve) shows that the negative electrode polarizes to ~-0.5V upon charge, then relaxes during the hold to 0.4V, showing that it is partially lithiated. The decrease in cell voltage (middle curve) upon discharge is seen to be mostly due to potential changes at the negative electrode, as expected from the anode-excess condition.

These cells were truly reversible and could be charged and discharged for 20 cycles with little change in behavior. The coulombic inefficiency seen in Fig. 3C and 3D is not unexpected, since it is well-known that passivation of graphite results in substantial irreversible consumption of lithium (10-15%) even in optimized lithium-ion batteries. Additional loss is attributed to cell imbalance; while the $LiCoO_2$/graphite mass ratio

theoretically provides equal Li storage capacity in the positive and negative electrodes (assuming charging of the positive electrode to the composition $Li_{0.5}CoO_2$), diffusion limitations prevent all of the Li in the $LiCoO_2$ from being utilized. Charging of the $LiCoO_2$ over 1-3h delithiates the surface of the densely sintered electrode to a depth of only a few micrometers given the relatively low chemical diffusion coefficient of Li at room temperature ($\sim 10^{-10}$ cm^2/s (*35*). This kinetic limitation causes the cells to be effectively have an excess of graphite, which could be readily corrected with a revised cell design.

These results demonstrate functional electrochemical junctions formed between lithium battery active materials under the influence of short-range repulsive forces alone, the formation of a percolating negative electrode network due to attractive interparticle forces, and adhesion of the graphite network to its metallic current collector, all occurring simultaneously within one solution phase. The result is a complete self-organized battery that can be repeatedly cycled. By using solid polymer electrolyte formulations that can be dried from solvent suspensions without losing the junctions therein, as was demonstrated between percolating ITO and graphite particle networks (*30*), fully solid-state batteries should be possible. Furthermore, use of anisometric particles (*18*) or the intrinsic anisotropy of crystalline materials to introduce orientation-dependent interactions could produce more complex device architectures than those discussed here. The present approach could potentially be applied to other devices or subcomponents of devices, including electrochemical sensors, electrochromic displays and windows, and particle-based solar cells such as those utilizing dye-sensitized nanoparticulate TiO_2 (*36*).

Experimental

Materials Preparation

$LiCoO_2$ powder was obtained from Seimi, and spherical graphitized mesocarbon microbeads (MCMB 6-28) was obtained from Osaka Gas Co., Japan. In order to prepare densely sintered $LiCoO_2$ electrodes, the powder was ball-milled with zirconia milling media in a zirconia jar mill in isopropanol for 24 hours, dried and pressed under 100 MPa pressure and sintered at 1100°C for 2 hours to form dense pellets with a density of 89 % that were then sectioned into bar-shaped samples. The lithium titanate reference electrode used in 3-electrode electrochemical cells was prepared by pressing and firing spinel powder (Altairnano, Reno, Nevada) at 1000°C for 2 hours, reaching density 92% of the theoretical value. Sections of the sintered sample were discharged to ~50% of capacity at C/12 rate against a lithium metal foil electrode in liquid electrolyte (1.33 M $LiPF_6$, EC:PC:DMC:EMC=4:1:2:2 by vol%) to reach a constant potential of 1.55 versus lithium determined by two-phase equilibrium. The highly-oriented pyrolytic graphite (HOPG, SPI 2-Grade) used as a substrate material was from Structure Probe, Inc., West Chester, PA. Other materials used were methylethyl ketone (2-Butanone, 99.5%, HPLC-grade, Sigma-Aldrich, Milwaukee, WI), acetonitrile (99.93%, HPLC-grade, Sigma-Aldrich, Milwaukee, WI), lithium perchlorate (99%, Alfa Aesar, Ward Hill, MA) and polyethylene glycol (PEG, MW 1500, Alfa Aesar, Ward Hill, MA).

Force Measurements

Contact mode AFM experiments were performed using a Nanoscope III instrument (Digital Instruments, Santa Barbara, CA). The colloid probes were prepared by mounting $LiCoO_2$ or MCMB particles of ~10 μm radius on the tip of Si_3N_4 cantilevers (Novascan Technologies, Ames, Iowa). The nominal spring constants of the cantilevers were 0.06 N/m. $LiCoO_2$ substrates were prepared by polishing the sintered disc (10 mm dia.) against SiC sandpapers and diamond abrasive papers down to 1 μm. All AFM probes and substrates were ultrasonicated in acetone and soaked in reagent grade methanol, n-heptane, and the test solvent, then dried thoroughly under vacuum. In the AFM experiments, the test fluid was introduced into the AFM fluid cell (Digital Instruments, Santa Barbara, CA) through Teflon tubing line and 0.2 μm filter (Pall Corporation, New York) by syringe and allowed to reach thermal equilibrium prior to the collection of force-separation data. Data was collected at a tip-to-substrate velocity of 50 nm/s or 200 nm/s.

Electrochemical testing

For construction of the self-organized electrochemical cells, the sintered $LiCoO_2$ pellets were sectioned to 10 × 6 × 2 mm dimensions for use as the positive electrode and drilled with a hole to attach a 0.254 mm platinum wire current collector. 0.28 g of the MCMB was used with 0.025mm thick platinum foil as the negative electrode current collector. Glass vials of 14 mm diameter and 45 mm height (VWR International, West Chester, PA, USA) were used to house the cells. All assembly and testing was conducted in an argon-filled glovebox (Labmaster 180, M.Braun, Stratham, NH) maintained at <0.1 ppm H_2O and O_2. The active materials, current collectors and glassware were dried at 60°C for 24

hours and soaked in the test solvent for several hours. Suspensions of the MCMB in the solvent mixture of interest were equilibrated in the vial prior to introduction of the positive electrode, and the cells were sealed to prevent solvent loss within the glovebox. The positive $LiCoO_2$ electrode was inserted into the settled and compacted MCMB powder bed to depths ranging from 1mm to 10mm during the tests of junction formation and electrochemical cycling. Both the two-electrode and three-electrode electrochemical tests were conducted using a potentiostat (SI 1287 electrochemical interface, Solarton Analytical, Hampshire, UK). All referenced potentials are reported vs. the Li/Li^+ couple.

References

1. A. Volta, "On the Electricity Excited by the Mere Contact of Conducting Substances of Different Kinds," *Phil. Trans. Royal Soc. London*, **90**, 403 (1800).
2. T. Rueckes, K. Kim, E. Joselevich, G.Y. Tseng, C.L. Cheung, C.M. Lieber, "Carbon Nanotube-Based Nonvolatile Random Access Memory for Molecular Computing," *Science* **289**, 94 (2000).
3. X. Duan, Y. Huang, Y. Cui, J. Wang, C.M. Lieber, "Indium Phosphide Nanowires as Building Blocks for Nanoscale Electronic and Optoelectronic devices," *Nature* **409**, 66 (2001).
4. I. Gur, N. A. Fromer, M. L. Geier, A. P. Alivisatos, "Air-Stable All-Inorganic Nanocrystal Solar Cells Processed from Solution," *Science* **310**, 462 (2005).
5. Y. Huang, X.F. Duan, Y. Cui, L. J. Lauhon, K.H. Kim, C. Lieber, "Logic gates and computation from assembled nanowire building blocks," *Science* **294**, 1313 (2001).
6. J.B. Bates, N.J. Dudney, B. Neudecker, A. Ueda, C.D. Evans, "Thin-film lithium and lithium-ion batteries," *Solid State Ionics*, **135**, 33 (2000).
7. M. Nathan, D. Golodnitsky, V. Yufit, E. Strauss, T. Ripenbein, I. Shechtman, S. Menkin, E. Peled, "Three-Dimensional Thin-Film Li-Ion Microbatteries for Autonomous MEMS,"
8. C.A. Vincent and B. Scrosati, *Modern Batteries:An Introduction to Electrochemical Power Source* (John Wiley & Sons, New York, 1997).
9. A. E. Curtright, P.J. Bouwman, R.C. Wartena and K.E. Swider-Lyons, "Power sources for nanotechnology," *Int. J. Nanotechnology* **1**, 226 (2004).

10. J.W. Long, B. Dunn, D.R. Rolison and H.S. White, "Three-Dimensional Battery Architectures," *Chem. Rev.* **104**, 4463 (2004).

11. M. Brouselly, "The Manufacturer's Point of View," Lithium Battery Discussion (LiBD), Arcachon, France, May 28, 2001.

12. W.D. Moorehead, *Concept and Feasibility Study for Self-Organized Electrochemical Devices* (MIT Thesis, Cambridge, MA, 2002) and Y.-M. Chiang, W.D. Moorehead, R.K. Holman, M.S. Viola, A.S. Gozdz, A. Loxley, G.N. Riley, Jr,, "Battery Structures, Self-Organizing Structures and Related Methods, Int. Patent App. WO03012908A2, published Feb. 13, 2003.

13. R. Wartena, A.E. Curtright, C.B. Arnold, A. Pique, K.E. Swider-Lyons, "Li-ion microbatteries generated by a laser direct-write method," *J. Power Sources*, **126**, 193 (2004).

14. R.M. Penner, C.R. Martin, *J. Electrochem. Soc.*, **133**, 310 (1986), and C.R. Martin, "Template synthesis of polymeric and metal microtubles", *Advanced Materials*, **3**, 457 (1991).

15. The micromanipulation of individual particles into such a configuration to form an aqueous battery has recently been described by Q.F. Shi and D.A. Scherson (*Electrochemical and Solid State Letters,* **8**, A122 (2005)). Here self-organization could be used to simultaneously form many such batteries in parallel.

16. R.W. Balluffi, S.M. Allen, W.C. Carter, *Kinetics of Materials* (John Wiley and Sons, New York, 2005).

17. G.R. Maskaly, R.E. Garcia, W.C. Carter, and Y.-M. Chiang, "Ionic Colloidal Crystals: Ordered, Multicomponent Structures via Controlled Heterocoagulation," *Phys. Rev. E*, in press.

18. T.D. Clark, J. Tien, D.C. Duffy, K.E. Paul and G.M. Whitesides, *J. Am. Chem. Soc.* **123**, 7677 (2001).

19. B.V. Derjaguin and L. Landau, "Theory of the Stability of Strongly Charged Lyophobic Sols and of the Adhesion of Strongly Charged Particles in Solutions of Electrolytes," *Acta Physicochim. URSS*, **14**, 633 (1941) and E.J.W. Verwey and J.Th.G. Overbeek, *Theory of Stability of Lyophobic Colloids* (Elsevier, Amsterdam, 1948).

20. For a general discussion see J.N. Israelachvili, *Intermolecular and Surface Forces, 2nd Edition* (Academic Press, London, U.K., 1992). See also: F. London, "The General Theory of Molecular Forces," *Trans. Faraday Soc.*, **33**, 8 (1937) and H.C. Hamaker, "The London-van der Waals Attraction between Spherical Particles," *Physica*, **4**, 1058 (1937).

21. A.W. Neumann, S.N. Omenyi, and C.J. van Oss, *Colloid and Polymer Sci.*, 257, 413-419 (1979).

22. C.J. van Oss, D.R. Absolom, and A.W. Neumann, *Colloids and Surfaces*, **1**, 45-56 (1980).

23. M. Morra and C. Cassinelli, *Colloids and Surfaces B-Biointerfaces* **18,** 249 (2000).

24. A.W. Neumann, *Advances in Colloid and Interface Science*, **4**, 105-191 (1974).

25. C.J. van Oss and A.W. Neumann, *Immunol. Commun.*, **6**(4) 341-354 (1977).

26. A. Milling, P. Mulvaney, and I. Larson, *J. Colloid and Interface Sci.*, **180,** 460 (1996).

27. S. Lee and W. M. Sigmund, "Direct Measurement of Repulsive van der Waals Interactions Using an Atomic Force Microscope," *J. Colloid and Interface Sci.*, **243,** 365 (2001).

28. For a review of methods for evaluating Hamaker constants see R.H. French, "Origins and Applications of London Dispersion Forces and Hamaker Constants in Ceramics," *J. Am. Ceram. Soc.*, ***83***, 2117 (2000).

29. E.M. Lifshitz, "The Theory of Molecular Attractive Forces between Solids," *Sov. Phys. JETP*, **2**, 73 (1956).

30. S.M. Tobias, *Investigation of Short-Range Surface Forces to Develop Self-Organizing Devices* (MIT Thesis, Cambridge, MA, 2005).

31. Since ITO also exhibits electrochromic darkening upon reduction, it could be an active electrode for self-organized electrochromic devices.

32. C. J. van Oss, R. J. Good, and M. K. Chaudhury, *Langmuir*, **4,** 884 (1988) and C. J. Van Oss, M. K. Chaudhury, and R. J. Good, *Chem. Rev.*, **88,** 927 (1988).

33. The OCV of 0.15-0.25V is as expected when there is no lithium salt in the solvent and therefore no discharge of the cell; only when the $LiCoO_2$ is delithiated and the graphite lithiated is the characteristic 3.6V voltage of a lithium-ion battery observed.

34. Control experiments were conducted in which the conductivity of the MCMB suspension in MEK containing 0.1M $LiClO_4$ and 1 wt % PEG 1500 was measured using Pt or HOPG as the current collectors. A low short-circuit resistance clearly indicated formation of an electronically conductive MCMB network. A second

control experiment tested the cell configuration in Fig. 3A in the absence of any solvent, and showed zero open circuit voltage (OCV) between the $LiCoO_2$ and MCMB, as expected for an electrically-shorted system.

35. Y.-I. Jang, B.J. Neudecker, N.J. Dudney, "Lithium Diffusion in Li_xCoO2 ($0.45<x<0.7$) Intercalation Cathodes," *Electrochem. Solid State Lett.*, **4**, A74 (2001).

36. M. Gratzel, "Photoelectrochemical Cells," *Nature*, **414**, 338 (2001).

List of Figures

Figure 1. Schemes for self-organization of bipolar electrochemical devices, using repulsive short-range forces such as the Lifshitz-van der Waals interaction (negative Hamaker constant, $A_{123}<0$) to form the electrochemical junction while simultaneously using attractive LW ($A_{121}>0$) to form percolating networks of a single active material and/or to selectively adhere to current collectors ($A_{123}>0$). A) Battery formed from a single particle pair. B) Nanorod-based batteries. C) Layered lithium-ion battery using repulsive short range forces to separate $LiCoO_2$ and graphite, while using LW attraction to form continuous percolating network of graphite anode. D) Interpenetrating electrode battery formed from a single heterogeneous colloid, wherein the electrodes form co-continuous percolating networks that are everywhere separated by repulsive force.

Figure 2. Colloid force results for MCMB graphite (top) and $LiCoO_2$ (bottom) tips as shown in F), measured against $LiCoO_2$ and graphite substrates in various solvent mixtures. A) Approach curves for MCMB tip against $LiCoO_2$ in MEK and MEK + 0.1M $LiClO_4$, showing smoothly repulsive interaction. B) Same tip and substrate in acetonitrile (AN) shows hysteresis between approach and retraction curves characteristic of adhesion. C) and D) In pure MEK, adhesive interactions are seen between MCMB tip and HOPG graphite, and $LiCoO_2$ tip and $LiCoO_2$ substrate, respectively, consistent with attractive LW interaction. E) Approach curves for MCMB tip against $LiCoO_2$ in MEK with and without PEG show that repulsive interaction is maintained.

Figure 3. Results for self-organized $LiCoO_2$-graphite rechargeable cells. A) Three-electrode cells using lithium metal or lithium titanate reference electrodes allowed

working voltage as well as the potentials at the working ($LiCoO_2$) and counter (MCMB graphite) electrodes to be independently measured. B) Open circuit potential between working and counter electrodes measured upon forcing $LiCoO_2$ electrode into contact with MCMB packed bed shows electrical short-circuit upon contact for acetonitrile, consistent with attractive interaction between the two electrode materials seen in Fig. 2B, but finite potential in MEK as repulsive surface forces, Fig. 2A, cause electrochemical junction to form between $LiCoO_2$ and graphite. C) Reversible galvanostatic cycling (50 μA) of self-organized battery using MEK + 0.1M $LiClO_4$ as the electrolyte. D) Measurements of potential difference between Li titanate reference electrode and the $LiCoO_2$ working (W) and MCMB counter (C) electrodes, conducted in MEK + 0.1M $LiClO_4$ + 1 wt% PEG 1500. Charging at 100 μA and discharging at 20 μA; all potentials referenced to Li/Li^+. Potentials observed during each stage of test demonstrate Faradaic activity, with the $LiCoO_2$ being delithiated and MCMB being lithiated.

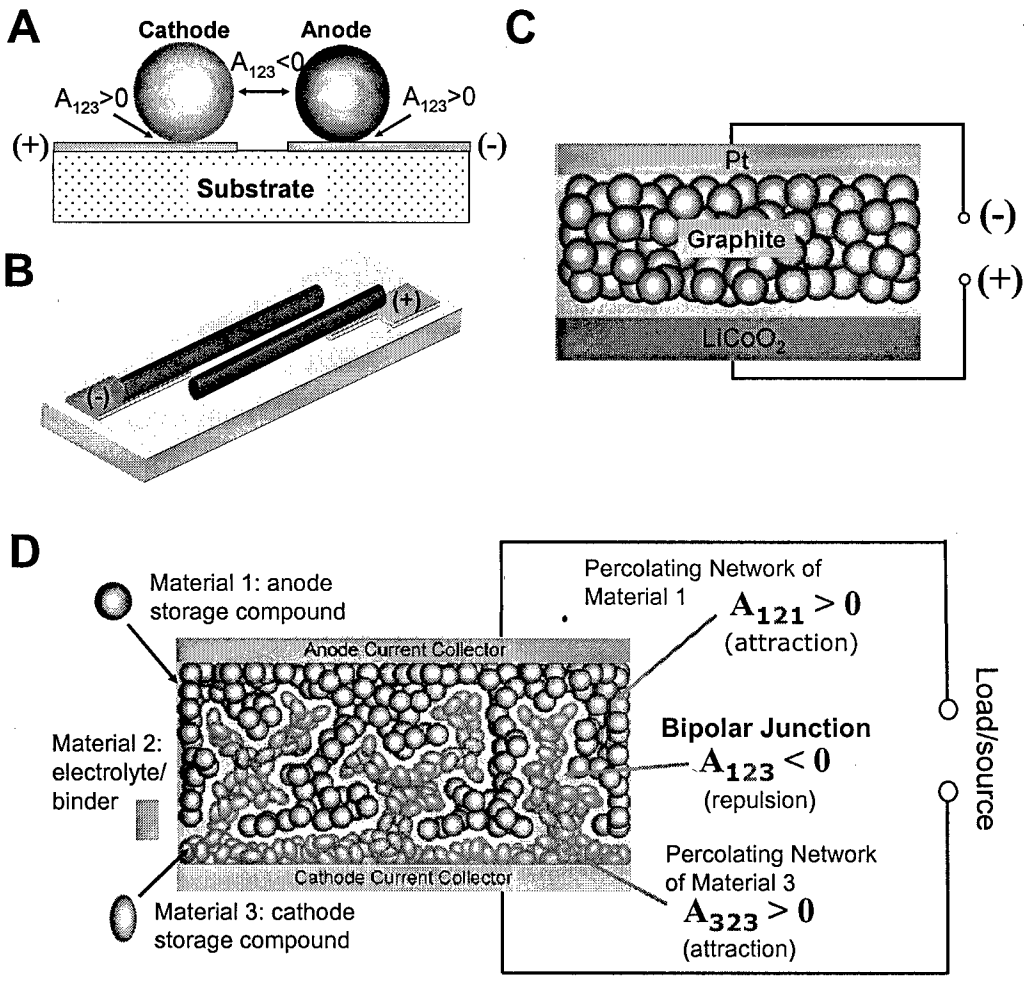

Figure 1. Schemes for self-organization of bipolar electrochemical devices, using repulsive short-range forces such as the Lifshitz-van der Waals interaction (negative Hamaker constant, $A_{123}<0$) to form the electrochemical junction while simultaneously using attractive LW ($A_{121}>0$) to form percolating networks of a single active material and/or to selectively adhere to current collectors ($A_{123}>0$). A) Battery formed from a single particle pair. B) Nanorod-based batteries. C) Layered lithium-ion battery using repulsive short range forces to separate $LiCoO_2$ and graphite, while using LW attraction to form continuous percolating network of graphite anode. D) Interpenetrating electrode battery formed from a single heterogeneous colloid, wherein the electrodes form co-continuous percolating networks that are everywhere separated by repulsive force.

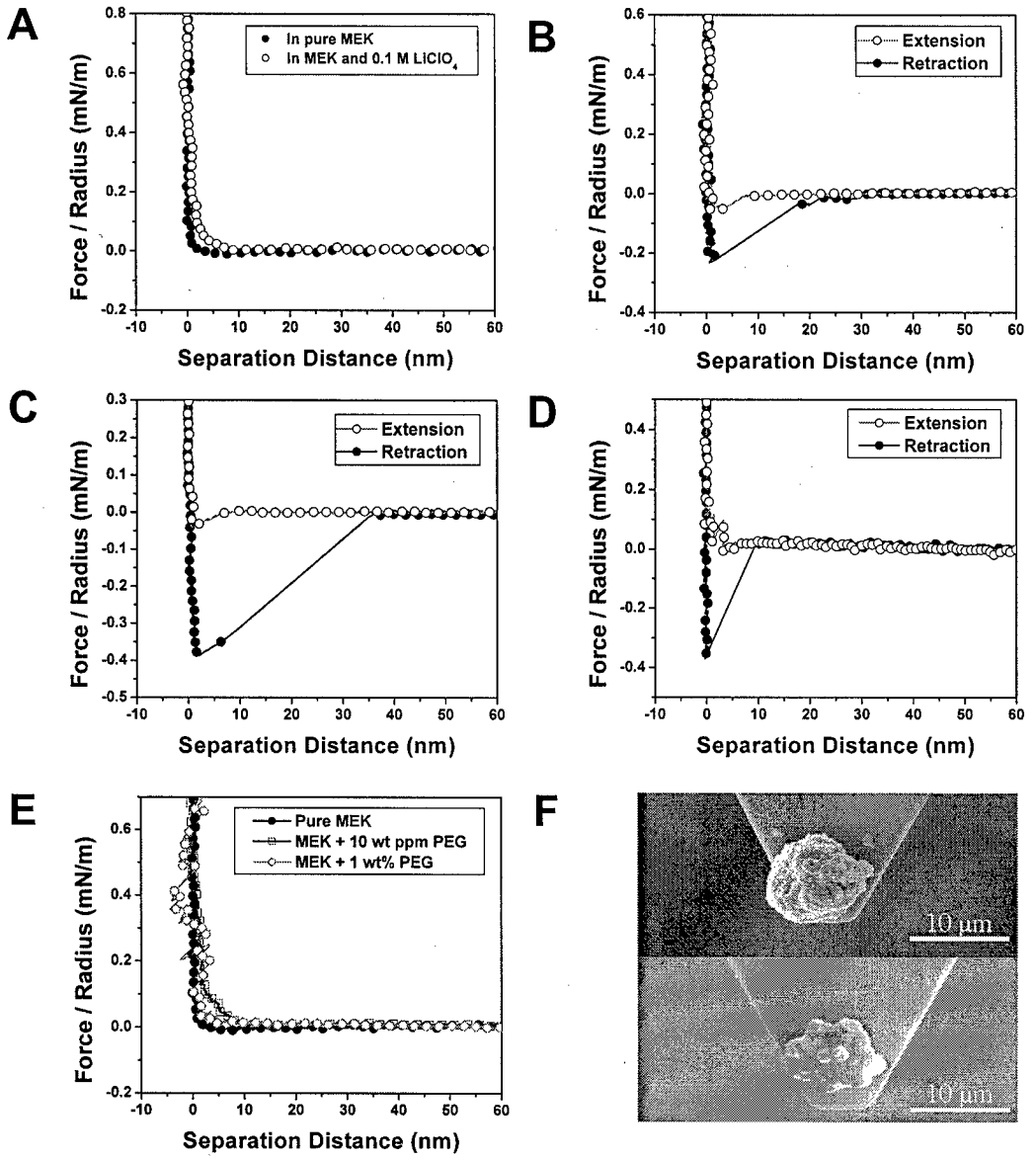

Figure 2. Colloid force results for MCMB graphite (top) and $LiCoO_2$ (bottom) tips as shown in F), measured against $LiCoO_2$ and graphite substrates in various solvent mixtures. A) Approach curves for MCMB tip against $LiCoO_2$ in MEK and MEK + 0.1M $LiClO_4$, showing smoothly repulsive interaction. B) Same tip and substrate in acetonitrile (AN) shows hysteresis between approach and retraction curves characteristic of adhesion. C) and D) In pure MEK, adhesive interactions are seen between MCMB tip and HOPG graphite, and $LiCoO_2$ tip and $LiCoO_2$ substrate, respectively, consistent with attractive LW interaction. E) Approach curves for MCMB tip against $LiCoO_2$ in MEK with and without PEG show that repulsive interaction is maintained.

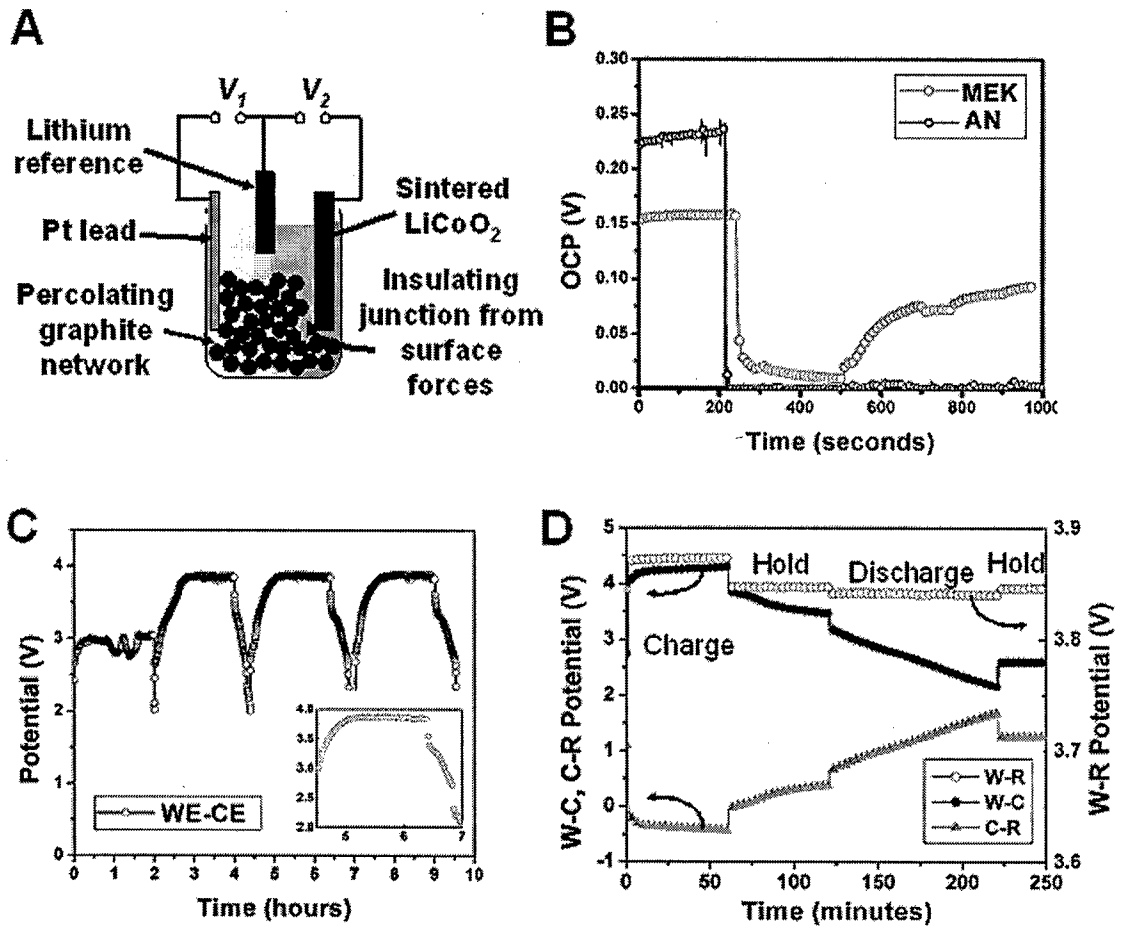

Figure 3. Results for self-organized $LiCoO_2$-graphite rechargeable cells. A) Three-electrode cells using lithium metal or lithium titanate reference electrodes allowed working voltage as well as the potentials at the working ($LiCoO_2$) and counter (MCMB graphite) electrodes to be independently measured. B) Open circuit potential between working and counter electrodes measured upon forcing $LiCoO_2$ electrode into contact with MCMB packed bed shows electrical short-circuit upon contact for acetonitrile, consistent with attractive interaction between the two electrode materials seen in Fig. 2B, but finite potential in MEK as repulsive surface forces, Fig. 2A, cause electrochemical junction to form between $LiCoO_2$ and graphite. C) Reversible galvanostatic cycling (50 μA) of self-organized battery using MEK + 0.1M $LiClO_4$ as the electrolyte. D) Measurements of potential difference between Li titanate reference electrode and the $LiCoO_2$ working (W) and MCMB counter (C) electrodes, conducted in MEK + 0.1M $LiClO_4$ + 1 wt% PEG 1500. Charging at 100 μA and discharging at 20 μA; all potentials referenced to Li/Li^+. Potentials observed during each stage of test demonstrate Faradaic activity, with the $LiCoO_2$ being delithiated and MCMB being lithiated.